Soft Matter

Cite this: *Soft Matter*, 2011, **7**, 5348

www.rsc.org/softmatter

PAPER

Facile one-pot preparation of novel shell cross-linked nanocapsules: inverse miniemulsion RAFT polymerization as an alternative approach†

Yin Wang,[ab] Guohua Jiang,*[ab] Ming Zhang,[ab] Lina Wang,[ab] Rijing Wang[ab] and Xinke Sun[ab]

Received 23rd December 2010, Accepted 25th March 2011
DOI: 10.1039/c0sm01534b

A series of novel shell cross-linked nanocapsules were facilely fabricated in an inverse miniemulsion reversible addition–fragmentation chain transfer (RAFT) system, in which poly(2-(dimethylamino) ethyl methacrylate) (PDMAEMA) acted as a stabilizer and macroinitiator. The as-prepared nanocapsules with PDMAEMA cores and poly(methylacrylic acid) (PMAA) shells, had a size of 220 nm and can be used as a carrier for the encapsulation of hydrophilic components such as inorganic salts.

1. Introduction

Great attention has been paid to the fabrication of nanocapsules due to their potential applications in diverse fields, such as in sensors, catalysis or pharmaceutics.[1–6] In addition, the majority of these applications greatly depend on the void space within the hollow structure of the nanocapsules, which can act as a "store-house" for catalysts, drugs, cosmetics, *etc.*[6] Thus, there has been considerable scope for the development of nanocapsules over the past decades.[7–16] One representative approach is to take advantage of sacrificial core templates.[9–12] In this approach, nanocapsules are usually synthesized by two steps: the core particles are first modified by single/multi polymeric shell(s), and then eliminated by a physical or chemical processes. The other promising method used to prepare nanocapsules appeals to soft temples including emulsion droplets[13,14] or vesicles,[15,16] which are stabilized by large amounts of surfactants. As for this approach, precursors are usually synthesized by polymerization *in situ* on the surface of the soft temples, then the liquid cores are removed by evaporation to produce nanocapsules. Though it is convenient to conduct these two approaches, relatively low preparation efficiency and tedious procedures to purify the resulting products have become a crucial issue to overcome in order to expand their practical applications. Fortunately, miniemulsion polymerization can circumvent these aforementioned limitations and can be easily scaled up to prepare nanocapsules.[17,18] However, miniemulsion polymerization cannot sufficiently incorporate hydrophilic substances into the core of nanocapsules at the beginning of the capsule formation process. Thus, it is urgent to instead use inverse miniemulsion polymerization, where the dispersed phase is a polar (water-soluble) monomer, which can greatly enhance the variety of applicable metal salts as well as the amount of the inorganic compound encapsulated.[19] For instance, Luo and coworkers prepared temperature sensitive nanocapsules which entrapped sodium sulfate by simply conducting inverse miniemulsion reversible addition–fragmentation chain transfer (RAFT) polymerization with poly(ethylene oxide)–MacroRAFT (PEO–RAFT).[20]

In practical applications, the stability of nanocapsules is a great challenge. One technique to achieve this goal is to cross-link the shells. However, the reported cross linkers are usually not cleavable.[8,21–23] Thus, if the cross linker is environment sensitive and cleavable, it would be more attractive. Matyjaszewski *et al.* reported the fabrication of redox sensitive shell cross-linked nanocapsules by means of electron transfer atom transfer radical polymerization (AGET ATRP) in a miniemulsion system.[24,25] Furthermore, to the best of our knowledge, there is not yet a report on the preparation of redox sensitive and shell cross-linked nanocapusles by inverse miniemulsion RAFT polymerization. The aim of the present work was to report a novel kind of shell cross-linked poly(2-(dimethylamino) ethyl methacrylate)-*b*-poly(methylacrylic acid) (PDMAEMA-*b*-PMAA) nanocapsules prepared using this methodology (Scheme 1). Then, these nanocapsules were used as a carrier to encapsulate sodium chloride.

2. Experimental

2.1 Materials

Ammonium persulfate (APS) and methylacrylic acid (MAA) were supplied by Tianjin Kermel Chemical Reagent Co., Ltd. (Tianjin, China) and used without further purification. Bis (acryloyloxyethyl) disulfide (BAEDS)[26,27] and poly(2-(dimethylamino)ethyl methacrylate) (PDMAEMA)[28] were prepared

[a]*Key Laboratory of Advanced Textile Materials and Manufacturing Technology (ATMT), Ministry of Education, Zhejiang Sci-Tech University, Hangzhou, 310018, P R China. E-mail: polymer_jiang@hotmail.com; Fax: +86 571 86843527; Tel: +86 571 86843527*
[b]*Department of Materials Engineering, College of Materials and Textile, Zhejiang Sci-Tech University, Hangzhou, 310018, P R China*
† Electronic supplementary information (ESI) available: detailed synthesis procedures and characterizations for shell cross-linked PDMAEMA-*b*-PMAA nanocapsules *via* inverse miniemulsion RAFT polymerization. See DOI: 10.1039/c0sm01534b

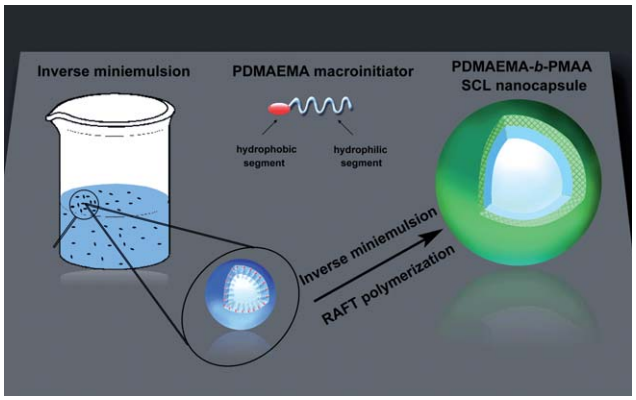

Scheme 1 A schematic representation of the fabrication of shell cross-linked PDMAEMA-*b*-PMAA nanocapsules *via* inverse miniemulsion RAFT polymerization.

according to literature procedures. Dithiothreitol (DTT), sorbitan monooleate (Span 80) and cyclohexane were used as received from Aladdin Reagent Co., Ltd. (Shanghai, China). MilliQ Water (18.2 MΩ cm^{-1}) generated from a Millipore MilliQ Academic Water Purification System was used throughout the experiments. All other reagents and solvents were of analytical grade and used as received without further purification.

2.2 Synthesis of shell cross-linked PDMAEMA-*b*-PMAA nanocapsules *via* inverse miniemulsion RAFT polymerization

Shell cross-linked PDMAEMA-*b*-PMAA nanocapsules (SCL nanocapsules) were fabricated by a one-pot method *via* inverse miniemulsion RAFT polymerization using PDMAEMA as the macroinitiator and stabilizing agent. A typical polymerization procedure is described as follows: a continuous phase comprised of an amount of cyclohexane, Span 80 (5 wt% relative to cyclohexane) and BAEDS (0.0524 g, 0.2 mmol) was vigorously stirred for 30 min and transferred to a dry flask. Meanwhile, PDMAEMA (0.0104 g, 0.01 mmol), APS (0.1369 g, 0.0006 mol), and MAA (0.25 mL, 2.2 mmol) were added to MilliQ Water (0.544 mL, 0.030 mol) to prepare the dispersed phase. After these two phases were mixed together, the reaction mixture was pre-emulsified at room temperature for 10 min, and sonicated for 180 s at 70% amplitude by an ultrasonic homogenizer (KQ-400KDE, Kunshan Ultrasonic Instrument Co., Ltd., China) in an ice-water bath to prevent the polymerization and evaporation of cyclohexane. Then, the prepared inverse miniemulsion was degassed by three cycles of freeze-pump-thaw procedure and flame-sealed under vacuum. Finally, the reaction was allowed to proceed in a pre-heated oil-bath at 60 °C for 24 h. Nanocapsules with non cross-linked shells have also been synthesized under the same condition except that the cross-linker, BAEDS, was not added into the reaction mixture.

After being cooled to the room temperature, an amount of the resulting solution was taken and centrifuged at a rate of 6000 rpm (TGL-16C, Shanghai Anting Scientific Instrument Factory, China), then washed with cyclohexane and water three times to remove any impurities. The obtained solid was lyophilized for 2–3 days before measurements were taken.

2.3 Cleavage of the SCL nanocapsules by DTT

The dried SCL nanocapsule powder (0.1 g) was dissolved in 10 mL DMF and transferred to a dry flask. Then, DTT (0.1 g, 0.154 mmol) was added. After being degassed by three cycles of freeze-pump-thaw procedure, the flask was immersed in an oil bath pre-heated to 50 °C, and the mixture was allowed to stir overnight. The colloid solution became clear, which means that the cross-linked structures were degraded into diblock copolymers after the addition of DTT. After dialysis of the solution for 1 day using a dialysis membrane with a molecular weight cutoff of 3500, the final degraded powder (PDMAEMA-*b*-PMAA-DTT) was obtained by lyophilization.

2.4 Encapsulation of sodium chloride into SCL nanocapsules *via* inverse miniemulsion RAFT polymerization

SCL nanocapsules containing sodium chloride (NaCl) were synthesized by adding various amounts of NaCl into the dispersed phase prior to the pre-emulsification of both phases. The amount of NaCl added to the dispersed phase was 0.01 g, 0.03 g, 0.05 g or 0.1 g. The rest of the procedures were the same as mentioned above.

2.5 Characterization

The ^{1}H NMR spectra were recorded on an AVANCE AV 400MHz Digital FT-NMR spectrometer operating at 400 MHz using deuterated DMSO-d_6 as the solvent. Gel permeation chromatographic (GPC) analysis was carried out at 40 °C. An Agilent 1100 series GPC system equipped with an LC pump, PL gel MIXED-C column, and RI detector was used. The column was calibrated with polystyrene standards of narrow molecular weight distribution. HPLC grade DMF was used as a mobile phase and the flow rate was 1.0 mL min^{-1}. The sizes and morphologies of the resultant samples were characterized by JSM-2100 transmission electron microscopy (TEM) equipped with an energy dispersive X-ray spectrum (EDXA, Inca Energy-200) at an accelerating voltage of 200 kV, whereby a small drop of sample solution was deposited onto a carbon-coated copper EM grid (200 mesh) and dried at room temperature at atmospheric pressure. Dynamic light scattering (DLS) measurements were performed in aqueous solution using a HORIBA Zetasizer apparatus (LB-550 V) equipped with a 5.0 mW laserdiode operating at 650 nm at room temperature. The measurements were conducted in quintuplicate. The results presented are the average of the data. In order to make each measurement comparable with another, the supernatant fluid of NaCl-containing SCL nanocapsules was taken for measurements. The supernatant fluid was prepared by allowing the reaction mixture to precipitate by gravity for 2–3 days. Thermogravimetric analysis (TGA) was performed on a Pyris Diamond 1 instrument (America) at a heating rate of 20 °C min^{-1} or 5 °C min^{-1} from 25 to 700 °C in a flow of nitrogen. Fourier transform infrared (FT-IR) spectra were recorded on a Nicolet 5700 spectrophotometer using an ATR cell or KBr pellets for samples.

3. Results and discussion

3.1 Synthesis of shell cross-linked PDMAEMA-*b*-PMAA nanocapsules *via* inverse miniemulsion RAFT polymerization

Inverse miniemulsion polymerization is a relatively new technique and has not been well studied. In addition, inverse

miniemulsion RAFT polymerization is an even more recent technique.[20,29] By combining RAFT polymerization with inverse miniemulsion, inverse miniemulsion RAFT polymerization is considered a powerful technique to synthesize unique or well-defined structured water-soluble copolymers or colloids such as nanocapsules.[20,29–31] As illustrated in Scheme 1, shell cross-linked PDMAEMA-*b*-PMAA nanocapsules can be facilely prepared by inverse miniemulsion RAFT polymerization in a one-pot method, using PDMAEMA as the macroinitiator and stabilizing agent. The mechanism is depicted in Scheme S1†.

GPC was used to investigate the molecular weight (M_n) and molecular weight distribution (M_w/M_n) of the polymers. The results are listed in Table 1. Compared to the M_n of the PDMAEMA sample, PDMAEMA-*b*-PMAA has a M_n of 37 459, indicating the successful chain extension of PDMAEMA. After being degraded by DTT, the PDMAEMA-*b*-PMAA-DTT has a molecular weight of 48 374. ^{1}H NMR was then used to characterize the structures of the polymers. In the case of PDMAEMA-*b*-PMAA, the peak at $\delta = 2.29$ ppm is assigned to the methyl group connected to the nitrogen (N–CH_3). Meanwhile, the proton peak at $\delta = 11.5$–12.5 ppm is attributed to the carboxyl groups of the PMAA blocks, which implies that PDMAEMA-*b*-PMAA has been successfully fabricated. As for the SCL nanocapsules, the peak ascribed to PDMAEMA disappears and the strength of the carboxyl groups peak decreases significantly, indicating that the shell of the nanocapsules has been fixed by BAEDS and the core is comprised by PDMEAMA. If the shell cross-linking was unsuccessful, dissociation into individual copolymer chains would be expected since DMSO-d_6 was a good solvent for the PDMAEMA and PMAA blocks, whose proton peaks could be observed (Fig. 1).

The compositions and thermal properties of the resultant nanocapsules were studied by Fourier transform infrared (FT-IR) and thermogravimetric analysis (TGA) (Fig. S1 and S2†). Both measurements show that PDMAEMA-*b*-PMAA nanocapsules have been successfully fixed by BAEDS. In order to obtain the size distributions of the nanocapsules, DLS measurements conducted in a cyclohexane dispersion were employed. As shown in Fig. 2, PDMAEMA-*b*-PMAA nanocapsules have an average hydrodynamic diameter of about 200 nm with a broad distribution range from 100 to 300 nm. Compared to the uncrosslinked nanocapsules, SCL nanocapsules have a slight larger average size, 224 nm with a low Span value which is used to characterize the size distribution of the samples. The calculated equation is shown in the ESI†. It can also be concluded from Fig. 2 that the proportion of nanocapsules with a size around 200 nm is higher than that of uncrosslinked ones, indicating that the shell cross-linked reaction may have a positive influence on the size distribution of the nanocapsules.

Table 1 Molecular weight and molecular weight distribution of polymers determined by GPC

	M_n/ g mol^{-1}	PDI
PDMAEMA	13 267	1.26
PDMAEMA-*b*-PMAA	37 459	1.14
PDMAEMA-*b*-PMAA-DTT	48 374	1.15

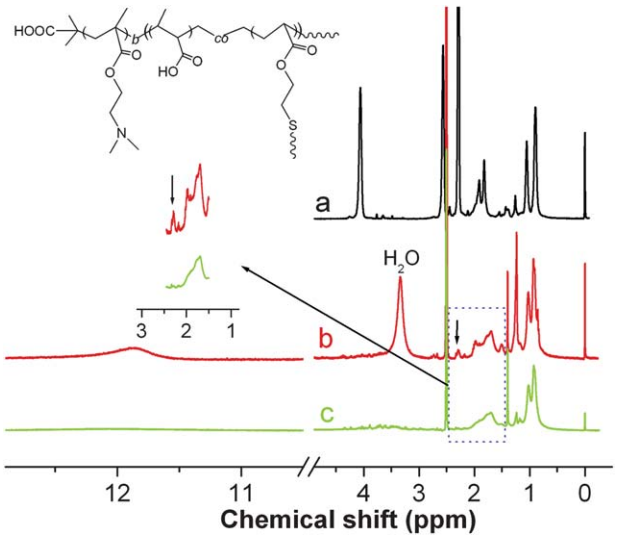

Fig. 1 ^{1}H NMR spectra of PDMAEMA (a), PDMAEMA-*b*-PMAA (b) and the SCL nanocapsules (c) in DMSO-d_6.

TEM was further used to investigate the morphology of the resultant nanocapsules. As shown in Fig. 3, the as-prepared samples consist of spherical nanocapsules and well-defined core–shell structures can be clearly observed. In the case of PDMAEMA-*b*-PMAA nanocapsules, the size is around 200 nm which is consistent with the DLS results and the thickness of the shell is around 30 nm. However, a great number of small fragments possibly derived from unstable nanocapsules can also be observed, which would give an undesirable contribution to the broad size distribution (Fig. 3a and b). As for the SCL nanocapsules, the diameter is about 220 nm, which is again in accord with the DLS results. Moreover, it can also be found from Fig. 3, that the as-prepared nanocapusles have preserved their spherical structure even after the drying process before the TEM measurement (Fig. 3c and d). The reasons for the above two phenomena are as follows: (i) the continuous phase, consisting of

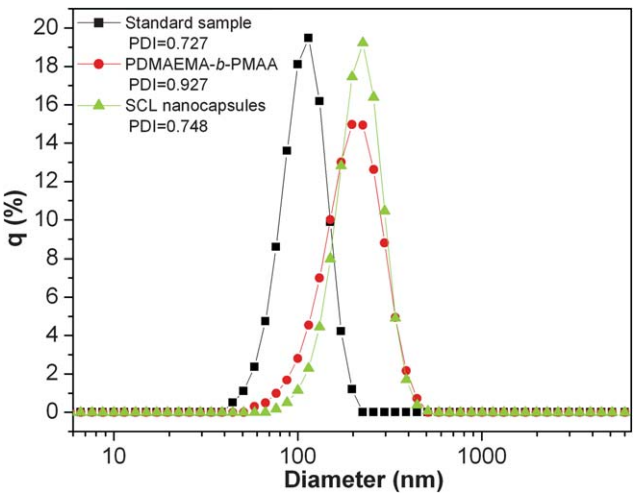

Fig. 2 Hydrodynamic diameter distributions of a standard sample, the PDMAEMA-*b*-PMAA nanocapsules and the SCL nanocapsules in dispersed in cyclohexane at 25 °C. The concentration of the samples is 1 mg mL^{-1}.

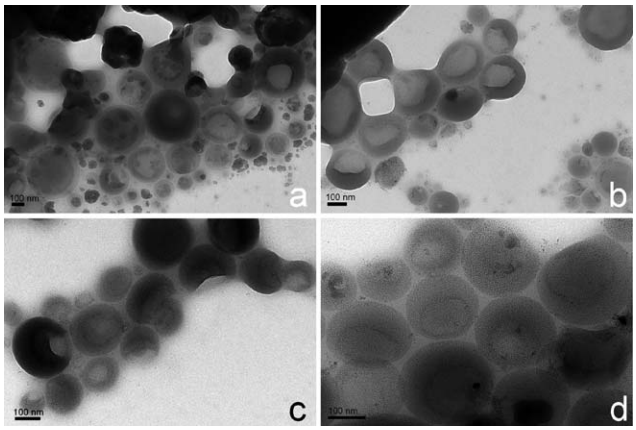

Fig. 3 TEM images of PDMAEMA-*b*-PMAA nanocapsules (a and b) and the SCL nanocapsules (c and d). All scale bars are 100 nm. The concentration of the samples is 1 mg mL^{-1}.

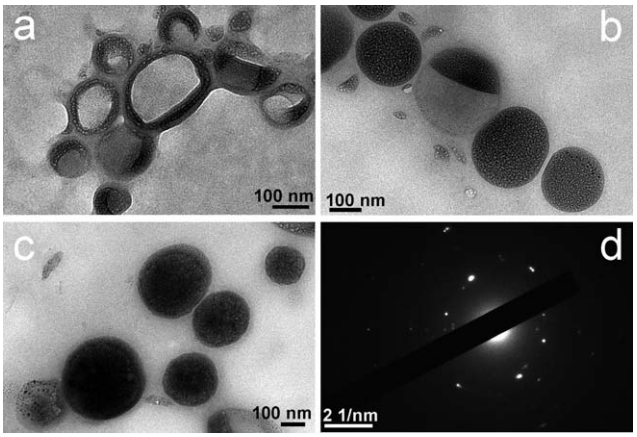

Fig. 4 Representative TEM images and electrical diffraction of sodium chloride-containing shell cross-linked PDMAEMA-*b*-PMAA nanocapsules. (d) is the corresponding electrical diffraction of (c). The concentration of the samples is 1 mg mL^{-1}. The amount of NaCl added into the dispersed phase is 0.03 g (a), 0.05 g (b) and 0.1 g (c).

cyclohexane and Span 80, are not good solvents for the PMAA shells. So the chains of PMAA tend to collapse easily on the surface of the PDMAEMA cores. That is, the DLS results would not reflect the contribution from the interaction between the PMAA shells and the aqueous dispersion. (ii) The impermeable shells of the nanocapsules also play an important role in the shape of the final capsules obtained by TEM. The less permeable the shells, the more difficult it is for the aqueous liquid to evaporate from the cores, and the easier it is for the shape to be preserved for the measurements. That the nanocapsules have impermeable shells is also confirmed by the FT-IR and TG results (Fig. S1 and S2†). In Fig. S1†, there is a broad shoulder peak between 3500 cm^{-1} and 3000 cm^{-1}, which can be assigned to the water entrapped in the nanocapsules. TGA curves also show that the resultant nanocapsules contain some water even after lyophilizing for 2–3 days before the measurement (Fig. S2†). Finally, the cross-linked networks also enhance the impermeability and rigidity of the shells,[22] which is good for the shape preservation.

3.2 Synthesis of NaCl-containing SCL nanocapsules *via* inverse miniemulsion RAFT polymerization

In order to provide evidence for one of the potential applications of the nanocapsules, NaCl as a model for the hydrophilic component was encapsulated into the nanocapsules. The morphology of the final colloids and the encapsulated inorganic salts were observed *via* TEM images and electrical diffraction, respectively. Spherical nanocapsules with a size of 200–300 nm can be observed in Fig. 4a–c and the void space within nanocapsules decreases as the amount of NaCl increases (more images are displayed in Fig. S3†). Moreover, it seems that when the amount of NaCl presented in the dispersed phase is at a larger scale, it's more difficult for the resultant nanocapsules to aggregate. This may be attributed to the function of NaCl which acts as co-stabilizer to reduce interfacial tension.[19] That is, the oil droplets would have better stability due to the presence of NaCl and do not easily aggregate or coalesce with others. The variation of Span values decreases also confirms that NaCl can improve the stability of the oil droplets (Fig. S4b†). Besides, a great number of seed-like dots can be found in void space of the SCL nanocapsules. These dots are confirmed to be crystalline structures from the electrical diffraction pattern as shown in Fig. 4d. In the present system, NaCl added into the dispersed phase should be the only thing present that could form crystals. Therefore, the encapsulated seed-like dots should be NaCl, which was salted out from the aqueous phase during the preparation of the TEM samples. The nature of the NaCl crystals were also confirmed by EDXA data, which is shown in Fig. S5†. Furthermore, as displayed in Fig. 4, the degree of crystallisation relies on the amount of NaCl added into the dispersed phase (the color of dots turns from colorless to black). This can be attributed to following reasons: when raising the amount of NaCl, the chance for each nanocaspsule to entrap inorganic salts increases and less water would be present in the void space. So it would be easier for NaCl to salt out during the TEM sample preparation process. Another reason may be attributed to the impermeable shells, which prevent the water evaporating from the cores and influence the degree of crystallisation. The electrical diffraction of NaCl with low crystal degree is displayed in Fig. S6†.

As reported, nanocapsules have extensively participated in drug delivery and control release systems, nevertheless, the controlled release of the molecules to a targeted area is the ultimate goal.[32–34] By introducing specific cleavable linkers to the shell of the nanocapsules, it should help to control the delivery of the encapsulated substances. For this purpose, BAEDS was chosen as the cross-linker, since the disulfide group can be cleaved to the corresponding thiols in the presence of reducing agents, such as tri(*n*-butyl) phosphine (Bu_3P),[35] dithiothreitol (DTT),[24,36] and glutathione.[37] In our case, the colloid solution of the SCL nanocapsules becomes clear under reductive conditions, indicating that the cross-linked structures were degraded (images inserted in Fig. 5). Furthermore, the successful cleavage of the disulfide linkages were also confirmed by the DLS results. As shown in Fig. 5, the diameter of the SCL nanocapsules in DMF is around 260 nm before degradation, which is larger than that in cyclohexane. This can be attributed to the fact that DMF is a good solvent for both PDMAEMA and PMAA, so the SCL

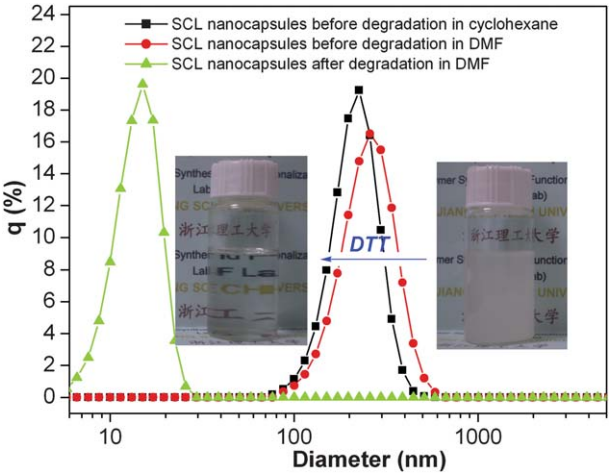

Fig. 5 Hydrodynamic diameter distributions and images of the SCL nanocapsule solution before and after adding DTT.

nanocapsules would swell spontaneously, resulting in an increase of the diameter. After degradation, the diameter decreases to 14.9 nm, indicating that the disulfide linkages have been cleaved sufficiently by DTT. This phenomenon is also reported by other research groups.[24,25,33] Related experiments of these SCL nanocapsules on drug delivery are now in progress, and the results will be presented in a separated paper.

4. Conclusion

A series of shell cross-linked PDMAEMA-*b*-PMAA nanocapsules were successfully fabricated *via* inverse miniemulsion RAFT polymerization at the interface between the oil droplets and water phase for the first time. The as-prepared shell cross-linked capsules have a size of 220 nm with a relatively narrow size distribution and can be used as a carrier to encapsulate the hydrophilic components including hydrophilic pigments, drugs or cosmetics, *etc.* The use of a cross-linker can improve the stability and impermeability of the final capsules through the formation of the cross-linked shells. In addition, it will also enhance the properties of controlled drug delivery because of its intrinsic redox responsiveness.

Acknowledgements

This work was financially supported by the National Natural Science Foundation of China (20604024), the Natural Science Foundation of Zhejiang Province (Y4100045), the Scientific Research Foundation of Zhejiang Sci-Tech University (0901808-Y) the Qianjiang Talents Project of Zhejiang Province (2010R10023), the Scientific Research Foundation for Returned Scholars, Ministry of Education of China (1001603-C) and the Program for Changjiang Scholars and Innovative Research Team in University (PCSIRT: 0654). YW thanks the Innovative Program for Graduate Students of Zhejiang Sci-Tech University through grant YCX-S11006. We greatly thank Qing Ye for 3D drawing and Rui Zhang for DLS measurements.

Notes and references

1 L. Y. Chu, T. Yamaguchi and S. Nakao, *Adv. Mater.*, 2002, **14**, 386–389.
2 S. Yang, Y. Zhang, G. Yuan, X. Zhang and J. Xu, *Macromolecules*, 2004, **37**, 10059–10062.
3 G. Sukhorukov, A. Fery and H. Möhwald, *Prog. Polym. Sci.*, 2005, **30**, 885–897.
4 L. Xie, M. Chem and L. Wu, *J. Polym. Sci., Part A: Polym. Chem.*, 2009, **47**, 4919–4926.
5 K. Landfester, *Angew. Chem., Int. Ed.*, 2009, **48**, 4488–4507.
6 X. W. Lou, L. A. Archer and Z. C. Yang, *Adv. Mater.*, 2008, **20**, 3987–4019.
7 S. Sugihara, S. P. Armes and A. L. Lewis, *Angew. Chem.*, 2010, **122**, 3578–3581.
8 C. Cheng, K. Qi, E. Khoshdel and K. L. Wooley, *J. Am. Chem. Soc.*, 2006, **128**, 6808–6809.
9 C. Boyer, M. R. Whittaker, C. Nouvel and T. P. Davis, *Macromolecules*, 2010, **43**, 1792–1799.
10 H. Gao, W. Yang, K. Min, L. Zha, C. Wang and S. Fu, *Polymer*, 2005, **46**, 1087–1093.
11 Z. Q. Shi, Y. F. Zhou and D. Y. Yan, *Polymer*, 2006, **47**, 8073–8079.
12 T. Kida, M. Mouri and M. Akashi, *Angew. Chem., Int. Ed.*, 2006, **45**, 7534–7536.
13 J. Jang and H. Ha, *Langmuir*, 2002, **18**, 5613–5618.
14 X. D. He, X. W. Ge, H. R. Liu, M. Z. Wang and Z. C. Zhang, *Chem. Mater.*, 2005, **17**, 5891–5892.
15 M. P. Krafft, L. Schieldknecht, P. Marie, F. Giulieri, M. Schmutz, N. Poulain and E. Nakache, *Langmuir*, 2001, **17**, 2872–2877.
16 J. Hotz and W. Meier, *Langmuir*, 1998, **14**, 1031–1036.
17 M. Antonietti and K. Landfester, *Prog. Polym. Sci.*, 2002, **27**, 689–757.
18 J. M. Asua, *Prog. Polym. Sci.*, 2002, **27**, 1283–1346.
19 E. Kobitskaya, D. Ekinci, A. Manzke, A. Plettl, U. Wiedwald, P. Ziemann, J. Biskupek, U. Kaiser, U. Ziener and K. Landfester, *Macromolecules*, 2010, **43**, 3294–3305.
20 F. J. Lu, Y. W. Luo, B. G. Li, Q. Zhao and F. J. Schork, *Macromolecules*, 2010, **43**, 568–571.
21 K. H. Bae, Y. Lee and T. G. Park, *Biomacromolecules*, 2007, **8**, 650–656.
22 E. Rosenbauer, K. Landfester and A. Musyanovych, *Langmuir*, 2009, **25**, 12084–12091.
23 G. Baier, A. Musyanovych, M. Dass, S. Theisinger and K. Landfester, *Biomacromolecules*, 2010, **11**, 960–968.
24 W. W. Li, K. Matyjaszewski, K. Albrecht and M. Möller, *Macromolecules*, 2009, **42**, 8228–8233.
25 W. W. Li, J. A. Yoon and K. Matyjaszewski, *J. Am. Chem. Soc.*, 2010, **132**, 7823–7825.
26 Y. T. Li and S. P. Armes, *Macromolecules*, 2005, **38**, 8155–8162.
27 L. Zhang, W. G. Liu, L. Lin, D. Y. Chen and M. H. Stenzel, *Biomacromolecules*, 2008, **9**, 3321–3331.
28 Y. Wang, G. H. Jiang, X. K. Sun, M. J. Ding, H. Y. Hu and W. X. Chen, *Polym. Chem.*, 2010, **1**, 1638–1643.
29 G. G. Qi, B. Eleazer, C. W. Jones and F. J. Schork, *Macromolecules*, 2009, **42**, 3906–3916.
30 G. G. Qi, C. W. Jones and F. J. Schork, *Macromol. Rapid Commun.*, 2007, **28**, 1010–1016.
31 L. Ouyang, L. S. Wang and F. J. Schork, *Macromol. Chem. Phys.*, 2010, **211**, 1977–1983.
32 G. J. Liu, S. B. Ma, S. K. Li, R. Cheng, F. H. Meng, H. Y. Liu and Z. Y. Zhong, *Biomaterials*, 2010, **31**, 7575–7585.
33 X. Z. Jiang, S. Y. Liu and R. Narain, *Langmuir*, 2009, **25**, 13344–13350.
34 K. Y. Pu, K. Li, J. B. Shi and B. Liu, *Chem. Mater.*, 2009, **21**, 3816–3822.
35 J. K. Oh, C. B. Tang, H. F. Gao, N. V. Tsarevsky and K. Matyjaszewski, *J. Am. Chem. Soc.*, 2006, **128**, 5578–5584.
36 H. L. Sun, B. N. Guo, R. Cheng, F. H. Meng, H. Y. Liu and Z. Y. Zhong, *Biomaterials*, 2009, **30**, 6358–6366.
37 J. K. Oh, D. J. Siegwart, H. Lee, G. Sherwood, L. Peteanu, J. O. Hollinger, K. Kataoka and K. Matyjaszewski, *J. Am. Chem. Soc.*, 2007, **129**, 5939–5945.

